Rapid Reaction Analysis of the Catalytic Cycle of the *Eco*RV Restriction Endonuclease[†,‡]

Geoffrey S. Baldwin, I. Barry Vipond, and Stephen E. Halford*

Department of Biochemistry, Centre for Molecular Recognition, University of Bristol, Bristol BS8 1TD, U.K.

Received July 19, 1994; Revised Manuscript Received October 28, 1994[⊗]

ABSTRACT: We have used the intrinsic tryptophan fluorescence of the *Eco*RV restriction endonuclease to monitor changes in protein conformation during binding and cleavage of a duplex oligodeoxynucleotide substrate. Appropriate conditions for single-turnover reactions were first determined by steady-state kinetics. When single turnovers were monitored by stopped-flow fluorescence, the mixing together of *Eco*RV, oligonucleotide and $MgCl_2$ resulted in a rapid increase in tryptophan fluorescence followed by a slow decrease. Further analysis by order-of-mixing and quench experiments showed that the transient increase in fluorescence was due to a conformational change coupled to DNA binding, while the subsequent decay was concomitant with phosphodiester hydrolysis. The rate of the latter step varied with the concentration of Mg^{2+} ions, but another Mg^{2+}-dependent transition was observed upon the addition of $MgCl_2$ to a preformed enzyme−DNA complex. These results lead to a reaction scheme in which one Mg^{2+} binds to the active site prior to phosphodiester hydrolysis but a second Mg^{2+} is then needed to carry out the hydrolytic reaction. This scheme is correlated to the crystal structures of the *Eco*RV endonuclease and its complexes with DNA and Mg^{2+} ions.

The two preceding papers (Kostrewa & Winkler, 1995; Vipond et al., 1995) present new data on the structure of the *Eco*RV restriction endonuclease and on its interactions with the divalent metal ions that it needs for DNA cleavage. These reports were preceded by a number of earlier studies on this enzyme [reviewed by Halford et al. (1993) and by Vipond and Halford (1993)]: X-ray crystallography on the free protein and its complexes with either specific or nonspecific DNA in the absence of Mg^{2+} (Winkler, 1992; Winkler et al., 1993); DNA binding equilibria (Taylor et al., 1991; Thielking et al., 1992); DNA cleavage specificity (Taylor & Halford, 1989, 1992; Vermote & Halford, 1992); nucleotide and phosphate analogs (Newman et al., 1990a,b; Grasby & Connolly, 1992; Jeltsch et al., 1993; Waters & Connolly, 1994); site-directed mutagenesis (Thielking et al., 1991; Vermote et al., 1992; Selent et al., 1992). However, almost all previous measurements of DNA cleavage by *Eco*RV were made under steady-state conditions and thus yielded comparatively little information about the intermediates in the reaction pathway. We describe here an analysis of the catalytic cycle of *Eco*RV by rapid-reaction techniques.

The substrate for stopped-flow experiments was a 12 bp[1] DNA duplex made from a palindromic oligodeoxynucleotide, GACGATATCGTC. It contains the *Eco*RV recognition site, GAT↓ATC, where ↓ marks the point of cleavage (Schildkraut et al., 1984; D'Arcy et al., 1985). This particular substrate was chosen because it has already been tested with *Eco*RV (Newman et al., 1990a,b; Waters & Connolly, 1992, 1994). It has a T_m of 53 °C (Newman et al., 1990a) and is thus double-stranded under all conditions used here. Cleavage of this DNA can be detected by quenching samples taken from the reaction at timed intervals and then separating the hexanucleotide products from the dodecanucleotide substrate by HPLC (Newman et al., 1990a). Its cleavage can also be monitored in a UV spectrophotometer by the hyperchromic shift assay (Waters & Connolly, 1992). The latter stems from the 6 bp products melting to single strands at temperatures where the 12 bp substrate remains double-stranded. We have used the resultant change in UV absorbance to follow the progress of both steady-state and single-turnover reactions. But our principal means for observing rapid reactions has been from changes in the tryptophan fluorescence of *Eco*RV (Baldwin & Halford, 1994).

In the complexes of *Eco*RV with either cognate or noncognate DNA, the DNA is held in a deep cleft between the two subunits of the dimeric protein (Winkler et al., 1993; Kostrewa & Winkler, 1995). *Eco*RV has four tryptophan residues per subunit, but none of these are on the DNA−protein interface nor are any near the active site. Instead, they are located either in the interior of the protein or on the external surface diametrically opposite the DNA-binding cleft. Consequently, any change in the intrinsic fluorescence of *Eco*RV upon binding or cleaving DNA is likely to be due to a conformational change in the protein that alters the environment of one or more of these distant tryptophans. The structure of the free *Eco*RV protein differs from that bound to nonspecific DNA, and it differs again when bound to specific DNA (Winkler et al., 1993). The *Eco*RV protein thus has several distinct conformations, but, as yet, nothing is known about the interconversions of these states. Hence, one purpose of the stopped-flow studies described here was to utilize the tryptophan fluorescence of *Eco*RV to report on the conformational changes during the course of the reaction.

[†] This work was supported by the Science and Engineering Research Council and the Wellcome Trust.

[‡] The submissions to the Brookhaven Protein Data Bank, 5RVE, 6RVE, and 7RVE, have been renamed by the Protein Data Bank as 1RVA, 1RVB, and 1RVC, respectively.

* Correspondence to this author. Phone: +44-(0)117-9-287429. Fax: +44-(0)117-9-288274.

[⊗] Abstract published in *Advance ACS Abstracts,* December 1, 1994.

[1] Abbreviations: bp, base pair(s); HPLC, high-performance liquid chromatography; K_D, equilibrium dissociation constant; PDB, (Brookhaven) Protein Data Base; T_m, melting temperature.

0006-2960/95/0434-705$09.00/0

EXPERIMENTAL PROCEDURES

Enzyme Purification. The *Eco*RV restriction endonuclease was purified as described previously (Luke et al., 1987) except that the ≥90% pure enzyme was now stored at 4 °C as a slurry in ammonium sulphate (80% saturated). Prior to each set of experiments, the enzyme was recovered from the slurry by centrifugation, dissolved in 50 mM Tris-HCl (pH 7.5), 100 mM NaCl, and 0.1 mM spermine, and dialyzed overnight against the same buffer. Protein concentrations were determined by OD_{280} with an extinction coefficient of 1.04×10^5 M^{-1} cm^{-1} (D'Arcy et al., 1985) where M refers to the molarity of the dimeric protein.

HPLC. Reverse-phase HPLC was performed on a Spectra Physics P4000 system fitted with a UV1000 detector set at 254 nm, a SP4290 peak integrator and a Hichrom NC300-5C18-250A octadecyl column thermostatted at 50 °C. Gradients were developed using 0.1 M triethylammonium acetate (pH 6.5) with 5% acetonitrile (buffer A) and 0.1 M triethylammonium acetate (pH 6.5) with 65% acetonitrile (buffer B), at a flow rate of 1 mL/min.

Oligodeoxynucleotide Synthesis and Purification. The oligodeoxynucleotide GACGATATCGTC was synthesized on a Du Pont CODER 300 DNA synthesizer with reagents from Cruachem. After deblocking with ammonia, the dimethyltrityl oligonucleotide was purified by reverse-phase HPLC using a 20−50% gradient of buffer B over 15 min. Solvents were removed from the pooled fractions by evaporation and the trityl group released by stirring with 80% acetic acid for 30 min. The acetic acid was removed by coevaporation with water, and the oligonucleotide was then dialyzed against 20 mM Tris-HCl (pH 7.5) and 100 mM NaCl, using Spectra Por cellulose ester membrane (2000 MW cut-off). The substrate was annealed by heating to 70 °C followed by cooling to 20 °C overnight. Concentrations were determined by OD_{254} with an extinction coefficient of 1.66×10^5 M^{-1} cm^{-1} for the duplex (Newman et al., 1990a).

Steady-State Kinetics. Reactions were generally carried out in 1-mL cuvettes at 25 °C in TN buffer (50 mM Tris-HCl, pH 7.5, 100 mM NaCl) containing the indicated concentrations of $MgCl_2$. Concentrations of the duplex oligodeoxynucleotide were varied from 0.05 to 5 μM. The reactions were initiated by adding 2 μL of the enzyme solution to give a final concentration of 1 or 2 nM *Eco*RV. The progress of the reaction was measured by following the increase in OD_{260} (Waters & Connolly, 1992) with a Perkin Elmer λ2 spectrophotometer. Reaction velocities were determined by computer-fitting to the initial linear portion of the increase in OD_{260} with time and were normalized for the variations in enzyme concentration.

Stopped Flow. Stopped-flow reactions were done in TN buffer, supplemented with $MgCl_2$ as required, at 25 °C (unless noted otherwise) in a Hi-Tech Scientific SF-51 apparatus. This device holds the two solutions of reactants in separate syringes: we will call "mixing" the intermingling of equal volumes of the two solutions in the flow cell, which is completed in about 2 ms; "premixing" will refer to the composition of the solutions in each syringe. The concentrations of the reactants are given after mixing. The apparatus was equipped with a 100-W mercury−xenon light source and a variable wavelength monochromator. Tryptophan fluorescence was excited at 290 nm and 90° emission observed through a Schott-Jena WG 320 cut-off filter, a set-up that excludes virtually all tyrosine fluorescence. Changes in absorbance were recorded with the same instrument but with the photomultiplier positioned at 180° to the light source. Both fluorescence and absorbance readings recorded with this instrument are given as relative values against an arbitrary offset of 1 V. Data were collected and analyzed with the Hi-Tech Scientific IS-1 software. The records shown are the averages from 3−12 consecutive repeats of each reaction.

At high light intensities, the *Eco*RV protein was found to undergo some photobleaching. This resulted in a small but progressive decrease in fluorescence intensity that continued for a much longer time than any of the reactions described here. The records from the reactions over long time bases (>1 s) have been corrected for this linear deviation: over short time bases (<1 s), the decrease in signal due to photobleaching was too small to detect.

Quench Assay. A reaction containing *Eco*RV (4 μM), oligodeoxynucleotide (2 μM), and $MgCl_2$ (1 mM) in 400 μL of TN buffer at 15 °C was initiated by the addition of the $MgCl_2$. Aliquots (20 μL) were removed from the reaction at 5 s intervals and mixed immediately with an equal volume of 0.5 M NaOH (Newman et al., 1990a). The quenched aliquots were stored on ice and analyzed as quickly as possible thereafter (to minimize degradation of the oligonucleotide). Analysis was by reverse-phase HPLC using a 5−15% gradient of buffer B over 15 min: the two hexanucleotide products eluted together, before the intact dodecanucleotide. The OD_{254} peaks from substrate and products, both single-stranded under the HPLC conditions, were integrated, and percent cleavage was determined from the ratio of the individual peaks to the total area.

Data Analysis. Data analyses and curve fitting for both steady-state and single-turnover experiments were by non-linear regression using GRAFIT (Erithacus Software, Slough, U.K.). The errors quoted are the standard deviations from the fitting procedures.

RESULTS AND DISCUSSION

Steady-State Analysis. The *Eco*RV restriction enzyme cleaves the duplex form of GACGATATCGTC, but, compared to plasmid substrates such as pAT153 (Taylor & Halford, 1989), this 12 bp DNA gives higher values for both k_{cat} and K_m (Newman et al., 1990b; Waters & Connolly, 1994). Single-turnover experiments demand that essentially all of the substrate present in the reaction mixture is bound to the enzyme, even when the concentration of the enzyme is only slightly higher than that of the substrate. Suitable conditions for single-turnover reactions, where the K_m for this substrate is sufficiently low to meet this requirement, were found by steady-state kinetics. The hyperchromic shift assay (Waters & Connolly, 1992) was used to provide a continuous spectrophotometric record of the cleavage of this oligonucleotide. At 25 °C, the substrate is double stranded while the products dissociate to single strands, thus leading to a measurable increase in OD_{260}. Steady-state rates were determined from the initial slope of OD_{260} against time. For each set of reaction conditions, the steady-state velocities were measured across a range of oligonucleotide concentrations. In all cases, the velocities showed a clean hyperbolic dependence on the concentration of the oligonucleotide (data

Table 1: Steady-State Kinetics[a]

$MgCl_2$ (mM)	NaCl (mM)	K_m (μM)	k_{cat} (s^{-1})
1	100	0.12 ± 0.02	0.13 ± 0.01
2	100	0.07 ± 0.01	0.28 ± 0.02
4	100	0.14 ± 0.02	0.43 ± 0.04
10	100	0.58 ± 0.06	0.70 ± 0.03
10	70	0.06 ± 0.01	0.66 ± 0.05

[a] Reactions were at 25 °C in 50 mM Tris-HCl (pH 7.5) with the concentrations of $MgCl_2$ and NaCl as indicated.

not shown), and values for K_m and k_{cat} were obtained by nonlinear regression fits to the Michaelis–Menten equation (Table 1).

Both k_{cat} and K_m for the oligonucleotide were evaluated at varied $MgCl_2$ concentrations in the presence of 100 mM NaCl. The values for k_{cat} increased with increasing concentrations of $MgCl_2$ while the values for K_m remained more or less constant at 0.1 ± 0.04 μM from 1 to 4 mM $MgCl_2$ (Table 1). At 10 mM $MgCl_2$, the K_m increased significantly, but this can be accounted for by the increased ionic strength from this amount of $MgCl_2$. When the NaCl concentration was reduced to 70 mM, to compensate for the ionic strength of 10 mM $MgCl_2$, the K_m returned to a lower value (Table 1). However, the ionic strength effects of Na^+ and Mg^{2+} on DNA–protein interactions differ from each other (Lohman, 1986), so all of the experiments described below were performed at low $MgCl_2$ concentrations (≤6 mM) with a constant level of 100 mM NaCl.

Our values for k_{cat} and K_m in 10 mM $MgCl_2$ and 100 mM NaCl agree closely with previous measurements under comparable conditions (Waters & Connolly, 1994).[2] They confirm the differences between this oligonucleotide and plasmid substrates. The reaction at the *Eco*RV site on pAT153 has a k_{cat} of about 0.015 s^{-1} at all concentrations of $MgCl_2$ tested (1–10 mM; Halford & Goodall, 1988), i.e., 10–50 times lower than those for the 12 bp substrate (Table 1). For the plasmid, the lack of variation in k_{cat} denotes saturation of the system with Mg^{2+}. For the oligonucleotide, the increase in k_{cat} with increasing levels of Mg^{2+} implies that the steady-state rate is coupled to the binding of Mg^{2+} and is limited by the fractional saturation with Mg^{2+}. The optimal K_m for this oligonucleotide is >100 times higher than that for pAT153 (Taylor & Halford, 1989), but its value of about 0.1 μM, at low concentrations of $MgCl_2$, is sufficiently small to ensure that essentially all of the substrate in single-turnover reactions with ≥2 μM *Eco*RV will be bound to the enzyme.

Stopped-Flow Fluorescence. The intrinsic tryptophan fluorescence of *Eco*RV was utilized in stopped-flow experiments to study DNA binding and DNA cleavage. The reactions were carried out with dimeric enzyme in excess of duplex oligonucleotide and with both reagents at concentrations that were at least 10 times higher than the K_m. The changes in fluorescence were monitored over a range of time bases, from 0.1 to 20 s, so that the formation and decay of the transient intermediates could be resolved (Figure 1).

[2] Some previous studies with GACGATATCGTC as the substrate for *Eco*RV had used the 5′-phosphorylated form of the oligodeoxynucleotide and these gave higher K_m values of about 3 μM, on account of the double negative charge on the 5′-phosphate (Newman et al., 1990b; Waters & Connolly, 1994). Only the unphosphorylated form was used here.

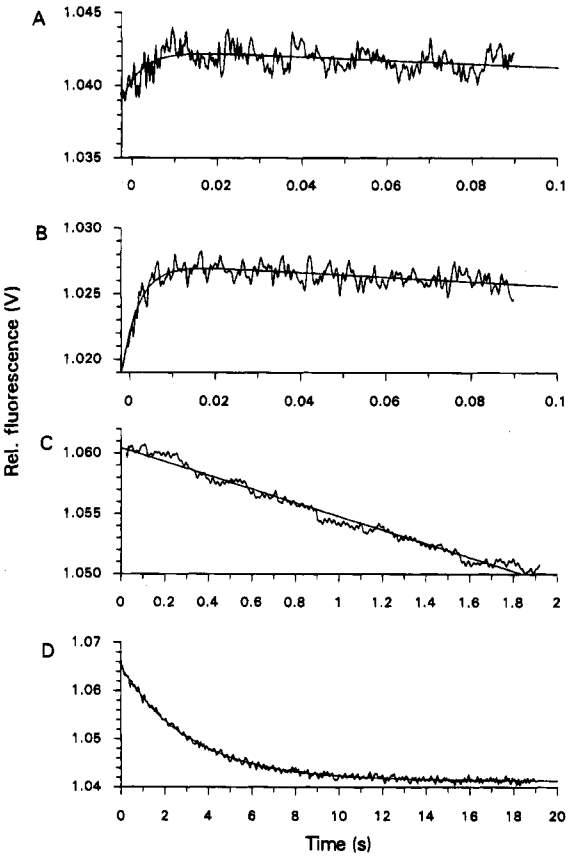

FIGURE 1: Stopped-flow fluorescence from *Eco*RV mixed with oligodeoxynucleotide. (Panel A) *Eco*RV in TN buffer at 25 °C was mixed by stopped-flow with oligodeoxynucleotide in the same buffer to give final concentrations of 4 μM *Eco*RV (dimer) and 2 μM oligonucleotide (duplex). The subsequent change in fluorescence was monitored for 0.1 s. The fluorescence record was fitted to an exponential increase, and the optimal fit, shown as a solid line through the data, was with k = 176 ± 19 s^{-1}. (Panels B–D) The reactions were identical to A except that both *Eco*RV and oligodeoxynucleotide solutions contained 1 mM $MgCl_2$. The record in B is over a 0.1 s time base, and the solid line is the optimal fit to an exponential increase in fluorescence (k = 244 ± 20 s^{-1}) followed by a linear decrease with time. The record in C is over a 2 s time base and was fitted to a linear decrease in fluorescence with time. The record in D is over a 20 s time base, and the solid line is the optimal fit to an exponential decrease in fluorescence (k = 0.26 ± 0.02 s^{-1}).

Following the mixing of the *Eco*RV enzyme with the 12 bp duplex in the absence of Mg^{2+}, an increase in the tryptophan fluorescence of the protein was observed (Figure 1A). At the concentrations of enzyme and DNA used here, the enhancement was complete within 20 ms, and no further changes in fluorescence were observed when the reaction was monitored over longer time bases (data not shown). However, the degree of enhancement was small compared to the overall fluorescence signal from the protein. The mixing of *Eco*RV and oligonucleotide in the absence of Mg^{2+} produced only a 0.5% enhancement in protein fluorescence. Consequently, the signal-to-noise ratios in the stopped-flow records from these binding reactions were too small for detailed kinetic analysis. [It was also too small for the equilibrium binding of the duplex to be measured by tryptophan fluorescence.]

Larger fluorescence signals were obtained during the catalytic cycle of *Eco*RV in the presence of Mg^{2+} (Figure 1B–D). The single-turnover reactions were carried out by

using the stopped-flow machine to mix (i) a solution containing both *Eco*RV and Mg^{2+} against a second containing both DNA and Mg^{2+}, (ii) *Eco*RV and Mg^{2+} against DNA, (iii) *Eco*RV against DNA and Mg^{2+}, and (iv) *Eco*RV premixed with DNA against Mg^{2+}.

Procedure (i) encompasses any effect that premixing with Mg^{2+} might have on either the enzyme or the oligonucleotide alone, but the results from procedures (ii) and (iii) were identical to (i), and only (i) is shown here (Figure 1B–D). However, the results from procedure (iv), with premixed *Eco*RV and DNA, were different and will be described later in this report (see below, Figure 4).

As with binding in the absence of Mg^{2+} (Figure 1A), the stopped-flow mixing of *Eco*RV, oligodeoxynucleotide, and Mg^{2+} generated a rapid increase in fluorescence over the first 20 ms of the reaction (Figure 1B), but this was now followed by a slow decay in the fluorescence signal over a 20 s time base (Figure 1D). No other process was observed at intermediate time scales (Figure 1C: the linear decrease in fluorescence shown in Figure 1C is simply the first 2 s of the process shown in full in Figure 1D). The rapid enhancement and the slow decay thus constitute all of the changes in protein fluorescence that occur during a single turnover of *Eco*RV, following the mixing of DNA and protein in the presence of Mg^{2+}.

When measured at the same concentrations of enzyme and DNA, the rate constant for the rapid increase in fluorescence in the presence of Mg^{2+} (Figure 1B) was similar to that from binding in the absence of Mg^{2+} (Figure 1A). This phase is thus likely to be associated with the binding of the enzyme to the DNA rather than any catalytic process. The apparent (first-order) rate constant for the formation of the high fluorescence transient was measured from single-turnover reactions at 2, 4, and 6 μM *Eco*RV: it increased progressively as the enzyme concentration was raised (data not shown). The pseudo-first-order rate constants measured over this range of enzyme concentrations yielded an average value of 5×10^7 M^{-1} s^{-1} for the second-order rate constant. Hence, this might appear to be a one-step binding process, occurring at a rate that is close to the diffusion-controlled limit for the association of a protein with a ligand (Fersht, 1985). However, since none of the tryptophans in *Eco*RV contact the DNA (Winkler et al., 1993), the enhancement in fluorescence may not be a direct consequence of DNA binding, and, instead, it could come from a conformational change linked to DNA binding.

Two sets of experiments were carried out in an attempt to establish whether the rapid increase in fluorescence was due to the bimolecular association with DNA or to a unimolecular rearrangement. First, the reactions were carried out at higher enzyme concentrations than those used above. A unimolecular step would have given a rate that showed a hyperbolic dependence on the concentrations of the reagents, while a bimolecular step would have given a rate that increased linearly with reagent concentration (Gutfreund, 1972). But it turned out to be impossible to extend these measurements to higher concentrations of *Eco*RV because the process was then too rapid to measure by stopped-flow. Second, the reactions at fixed concentrations of *Eco*RV, DNA, and $MgCl_2$ were studied at varied temperatures: the rate of the fluorescence enhancement doubled from 5 to 15 °C and doubled again from 15 to 25 °C. [It was impossible to extend these measurements to higher temperatures because the rates again became too fast to measure by stopped-flow.] The doubling in rates for 10 °C rises in temperature corresponds to an Arrenhius activation energy of about 12 kcal/mol. This contrasts with the activation energies that are generally found for diffusion-controlled bimolecular reactions, which are usually <3 kcal/mol (Gutfreund, 1972). We therefore tentatively assign the rapid increase in fluorescence to a unimolecular conformational change.

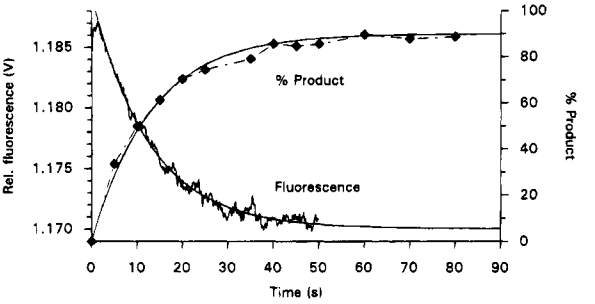

FIGURE 2: Single-turnover quench assay. Reactions at 15 °C contained *Eco*RV (4 μM), oligodeoxynucleotide (2 μM), and $MgCl_2$ (1 mM) in TN buffer. The reactions were initiated by the addition of $MgCl_2$. The progress of the reaction was monitored by either stopped-flow fluorescence (left-hand scale) or by the quench assay described in Experimental Procedures (right-hand scale). For the latter, aliquots were removed from the reaction at the times indicated and then quenched immediately in NaOH prior to analysis by HPLC. Product formation (% total DNA) at each time point is given as a diamond, and the solid line through this data is the optimal fit to a single-exponential increase ($k = 0.076 \pm 0.005$ s^{-1}). The solid line through the fluorescence data is the optimal fit to a single-exponential decrease ($k = 0.080 \pm 0.003$ s^{-1}).

Once formed, the high fluorescence transient decayed as a single-exponential (Figure 1D). The rate constant for the decay, 0.26 s^{-1}, was double the value of k_{cat} determined from the steady-state reactions at the same concentration of $MgCl_2$, 0.13 s^{-1} (Table 1). The turnover number of *Eco*RV must therefore be limited to some extent by the process that gives rise to the decay phase. The fluorescence decay is unlikely to be directly due to either phosphodiester hydrolysis or product release, since none of the tryptophans in *Eco*RV are near the active site (Winkler et al., 1993), but it could be due to a conformational change in the protein that is concomitant with either of these processes.

Phosphodiester Hydrolysis. In order to determine whether the decay phase in the stopped-flow fluorescence (Figure 1D) corresponds to DNA cleavage or to product release, a direct comparison was made between the fluorescence data and the conversion of the dodecanucleotide substrate into hexanucleotide products (Figure 2). The latter was measured by using NaOH to quench samples taken from a single-turnover reaction. The reaction was performed at 15 °C and 1 mM $MgCl_2$, so that the rate of cleavage was slow enough for the sampling to be done manually at 5 s intervals. Percentage product in each sample was determined by HPLC (Experimental Procedures). By denaturing *Eco*RV with NaOH (Newman et al., 1990a), the quench assay yields the rate of phosphodiester hydrolysis independently of product dissociation.

The quench assay gave an exponential curve for the increase in product, from which a first-order rate constant was calculated (Figure 2). Stopped-flow fluorescence experiments were performed under identical reaction conditions. The high fluorescence transient decayed exponentially with the same rate constant as that observed for the formation

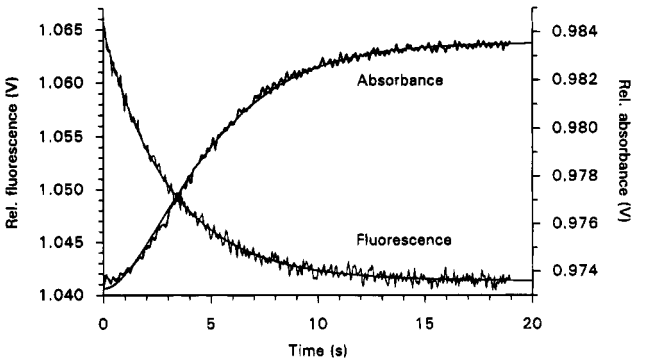

FIGURE 3: Absorbance and fluorescence from a single turnover. The stopped-flow device was used to mix *Eco*RV and $MgCl_2$ with oligodeoxynucleotide and $MgCl_2$, to give reaction mixtures containing 4 μM *Eco*RV, 2 μM duplex oligonucleotide, and 1 mM $MgCl_2$ in TN buffer at 25 °C. The progress of the reactions were monitored by either fluorescence (left-hand scale) or absorbance at 260 nm (right-hand scale). The solid line through the fluorescence data is the optimal fit to a single-exponential decay ($k = 0.26 \pm 0.004$ s^{-1}), and the solid line through the absorbance data is the fit to [C] in the two-step consecutive pathway, A $\rightarrow$ B $\rightarrow$ C: the optimal fit was obtained with values of 0.38 ± 0.04 and 0.39 ± 0.04 s^{-1} for the two rate constants.

of the hexanucleotide product (Figure 2). The decay of the high fluorescence transient thus occurs simultaneously with the hydrolysis of the phosphodiester backbone and is thus a signal for the formation of enzyme-bound product as opposed to product release.

The application of the quench assay to single turnovers of *Eco*RV also demonstrates that the only detectable product is DNA cleaved in both strands. If the reaction had proceeded by first cutting one strand to generate a nicked intermediate and only later the second strand, the quench assay would have given a biphasic record. Instead of one rate constant for the complete reaction (Figure 2), the rate constant for the first 50% would have been higher than that for the second 50%. Moreover, if nicked DNA had dissociated from the enzyme, the hexanucleotide products would separate from the intact dodecanucleotide strands and the latter would reanneal to regenerate the substrate, thus making the single-turnover kinetics much more complicated than the fluorescence records reported here. Our data on *Eco*RV contrast with the multiphasic kinetics observed by stopped-flow fluorescence on *Eco*RI, where single-turnover reactions produce initially a nicked intermediate that dissociates from the protein and which then gives rise to fresh substrate by the reannealing of intact strands (Alves et al., 1989). Our failure to detect nicked intermediates implies that *Eco*RV hydrolyzes the second strand of this 12 bp substrate at a faster rate than the first strand and that only the latter is measured here. This concurs with previous studies on the cleavage of supercoiled plasmids by *Eco*RV under similar reaction conditions, where no open circle DNA was detected (Halford & Goodall, 1988).

Product Dissociation. The hyperchromic shift assay (Waters & Connolly, 1992) used in the steady-state analysis was also employed for single-turnover reactions in a stopped-flow spectrophotometer (Figure 3). In single-turnovers, the hyperchromic shift should provide a direct signal for product release as opposed to product formation. Our rationale for this view is that, since the *Eco*RV endonuclease completely surrounds the DNA to which it is bound (Winkler et al., 1993), the 6 bp products formed from the 12 bp substrate would be unable to dissociate to single strands without first dissociating from the protein. Moreover, the crystal structure of the enzyme–product complex for *Eco*RV shows that 5 bp products remain double-stranded when bound to the enzyme, even though the co-crystallization was at 20 °C (Kostrewa & Winkler, 1995). Melting of 6 bp duplexes, the lengths of the products of this reaction, occurs in <1 ms under the conditions used here [by extrapolation from the data of Craig et al. (1971)]. Consequently, the increase in OD_{260} upon DNA melting should occur immediately after product dissociation.

When the same reaction of *Eco*RV and oligodeoxynucleotide was monitored in the stopped-flow at 25 °C by either OD_{260} or tryptophan fluorescence, an increase in OD_{260} was observed, over a similar time scale to the decay of the high fluorescence transient (Figure 3). However, a pronounced lag phase was observed at the start of the OD_{260} record: no equivalent lag phase was observed in the fluorescence record. [When the comparison between the OD_{260} and the fluorescence records was made with identical reactions at 15 °C rather than at 25 °C, the fluorescence signal was as shown in Figure 2 but no increase in OD_{260} was observed. The 6 bp products presumably remain double-stranded at 15 °C. The fluorescence signal therefore cannot be an artifact stemming from a change in the UV absorption of the reaction mixture.]

Since the fluorescence decay and the quench assay yield the same exponential (Figure 2), the rate of formation of the enzyme-bound product must be limited by just one step in the reaction mechanism and the rate constant for that step must be smaller than any other step in the pathway prior to the enzyme–product complex, i.e.,

$$E + S \xrightarrow{k_b} ES \xrightarrow{k_h} EP \qquad (1)$$

where k_h, the apparent rate constant for phosphodiester hydrolysis, is much smaller than k_b, the rate constant for the formation of ES. [For the reasons given above, ES and EP refer respectively to the DNA–protein complexes where neither or both strands have been cut, and k_h is the apparent constant for cutting the first strand: the rate constant for cutting the second strand is larger than k_h and cannot limit the formation of EP.] In contrast, the hyperchromic shift signals the dissociation of the product from the enzyme–product complex, i.e.,

$$ES \xrightarrow{k_h} EP \xrightarrow{k_r} E + P \qquad (2)$$

where k_r is the rate constant for product release. If k_h and k_r have similar values, then the formation of free product from this consecutive pathway will involve a lag phase. The assignments of the fluorescence decay to the formation of the enzyme–product complex and the kinetically distinct hyperchromicity to the formation of free product imply that the tryptophan fluorescence of the enzyme–product complex must be very similar to that from the free enzyme and that only the enzyme–substrate complexes have significantly enhanced fluorescence.

The rate equation for a two-step consecutive reaction (Fersht, 1985)[3] was fitted to the time course for the hyperchromic shift in Figure 3. The rate equation for a two-step pathway yields two rate constants, but it cannot

distinguish which constant refers to the first step and which to the second (Fersht, 1985). However, the fitting procedure gave similar values for the two constants, 0.38 and 0.39 s^{-1}, both of which were fairly close to the value for k_h determined from the same reaction by fluorescence, 0.26 s^{-1}. These values account quantitatively for the k_{cat} of *Eco*RV. If the turnover number is determined by the rate constants for both phosphodiester hydrolysis (k_h) and product release (k_r), then

$$k_{cat} = (k_h k_r)/(k_h + k_r) \quad (3)$$

so that, when $k_h = k_r$, $k_{cat} = k_h/2$. The latter agrees with the experimental value for k_{cat} under the same reaction conditions, 0.13 s^{-1} (Table 1). Under these conditions (1 mM $MgCl_2$), the steady-state rate for cleaving this oligonucleotide is determined by the rate constants for both product formation and product release. In contrast, the steady-state rate of *Eco*RV on plasmid substrates is not only much slower than that on the oligonucleotide, it is also limited solely by product release (Halford & Goodall, 1988). The lower value of k_{cat} with plasmids may be due to initial transfer to nonspecific DNA prior to dissociation, as has been suggested for *Eco*RI (Terry et al., 1987).

Premixed Enzyme–DNA Complex. Stopped-flow experiments were also carried out to observe the changes in tryptophan fluorescence following the addition of Mg^{2+} to a premixed solution of *Eco*RV enzyme and oligodeoxynucleotide (Figure 4). This mixing procedure (noted above as iv) produced a different response from the fluorescence signal compared to procedures i–iii, where separate solutions of *Eco*RV and oligonucleotide were mixed together in the presence of $MgCl_2$ (Figure 1). The rapid increase in fluorescence that had been observed over the first 20 ms of the reaction (Figure 1B) was no longer detected (Figure 4A). But an intermediate (2 s) time scale revealed an increase in fluorescence (Figure 4B) that had no counterpart in the reactions starting from the separate components (Figure 1C). The subsequent decay of fluorescence (Figure 4C) was unchanged from that observed previously (Figure 1D): it had the same rate constant regardless of the mixing procedure.

The *Eco*RV endonuclease binds DNA in the absence of Mg^{2+} (Taylor et al., 1991), so the reaction of premixed enzyme and DNA will start from the DNA–protein complex. This explains the absence of the rapid (20 ms) enhancement in fluorescence from the premixed solution (Figure 4A). This process has already been linked to the binding of the protein to DNA. But the addition of Mg^{2+} to the DNA–protein complex resulted in a distinct fluorescence enhancement on a 2 s time scale (Figure 4B). At the millimolar concentrations of $MgCl_2$ used here, the bimolecular step in binding Mg^{2+} will be complete within <0.1 ms (assuming a second-order rate constant of $\geq 1 \times 10^7$ M^{-1} s^{-1}), so this process is likely to reflect a comparatively slow Mg^{2+}-dependent conformational change in the enzyme–DNA complex prior to phosphodiester hydrolysis. In the structure of the enzyme–DNA complex in the absence of Mg^{2+} (Winkler et al., 1993),

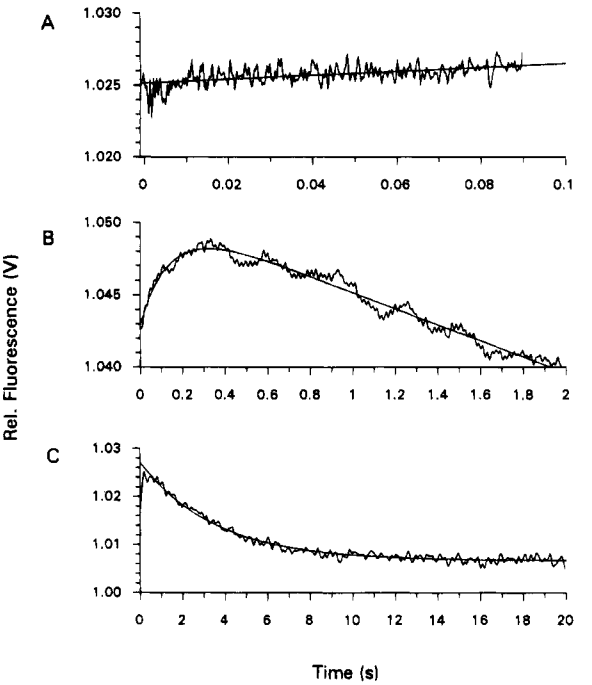

FIGURE 4: Stopped-flow fluorescence from *Eco*RV premixed with oligodeoxynucleotide. A solution of *Eco*RV and oligodeoxynucleotide in TN buffer at 25 °C was mixed by stopped-flow with $MgCl_2$ in the same buffer to give final concentrations of 4 μM *Eco*RV, 2 μM duplex oligonucleotide, and 1 mM $MgCl_2$. The subsequent changes in fluorescence was monitored over the time bases as indicated. The record in A is over a 0.1 s time base, and the solid line is the optimal fit to an linear increase in fluorescence (i.e., the first 0.1 s of the reaction in B). The record in B is over a 2 s time base and was fitted to an exponential increase in fluorescence ($k = 7.3 \pm 0.3$ s^{-1}) followed by a linear decrease. The record in C is over a 20 s time base, and the solid line is the optimal fit to an exponential decrease in fluorescence ($k = 0.28 \pm 0.02$ s^{-1}).

the binding sites for Mg^{2+} lie underneath the DNA and the DNA hinders access to these sites from bulk solution. Hence, it is reasonable to suggest that the *Eco*RV–DNA complex has to undergo a structural rearrangement to allow Mg^{2+} to bind. However, the absence of this phase when *Eco*RV binds to DNA in the presence of Mg^{2+} (Figure 1C) indicates that this particular Mg^{2+} ion is usually incorporated into the enzyme–DNA complex concurrently with DNA binding, possibly by prior coordination to the DNA phosphates.

The stable complex formed between *Eco*RV and DNA in the absence of Mg^{2+} is therefore not an obligatory intermediate in the direct pathway for a reaction starting with enzyme, substrate, and cofactor separate from each other. However, the 2 s fluorescence signal (Figure 4B) shows that the nonproductive enzyme–DNA complex formed in the absence of Mg^{2+} can join the reaction pathway by an alternative route. Moreover, the additional fluorescence enhancement, upon the incorporation of Mg^{2+} into the nonproductive enzyme–DNA complex (Figure 4B), explains why the fluorescence change observed on binding *Eco*RV to DNA in the absence of Mg^{2+} (Figure 1A) is less than that in the presence of Mg^{2+} (Figure 1B): the increase in Figure 1B is mechanistically equivalent to the sum of the increases in Figures 1A and 4B. The maximal enhancement of *Eco*RV fluorescence is obtained only when both DNA and Mg^{2+} are bound.

[3] The fit to a two-step consecutive reaction deviated slightly from the experimental record at the very start of the record (Figure 3). A possible explanation for this deviation is that the two-step scheme in eq 2 is an oversimplification and that the rate of formation of free product is limited by three or more steps with similar rate constants (Halford & Johnson, 1983).

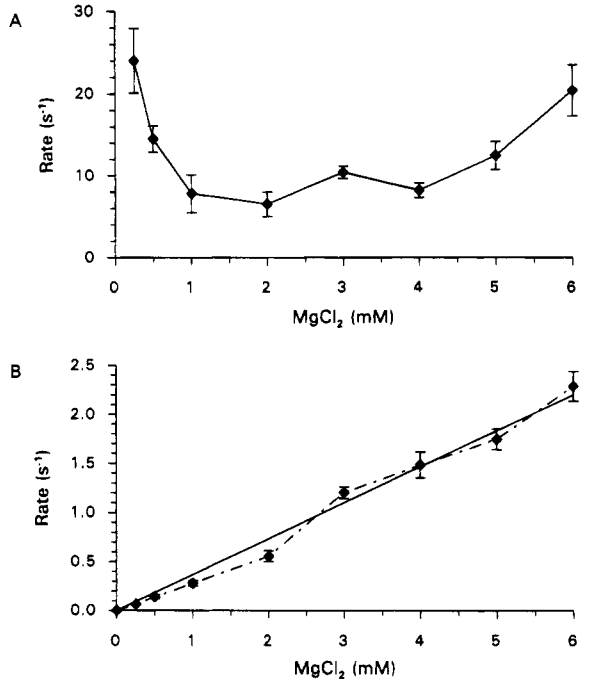

FIGURE 5: Mg^{2+} dependencies of the fluorescence transitions. (A) The rate constants for the intermediate phase of fluorescence enhancement, observed when the enzyme−oligodeoxynucleotide complex was mixed with Mg^{2+} (Figure 4B), were measured from reactions at 25 °C in TN buffer with 4 μM *Eco*RV, 2 μM duplex oligonucleotide, and at varied concentrations of $MgCl_2$ as shown. The line is drawn simply to connect the data points. (B) The rate constants from the fluorescence decay were measured from reactions containing the same concentrations of reagents as above. The dashed line connects the data points while the solid line is the optimal fit for a linear increase in rate with increasing concentrations of $MgCl_2$. In both panels, the error bars on all data points indicate the range of values from repeat experiments.

Mg^{2+} Dependencies. Our stopped-flow fluorescence studies have revealed three conformational changes in the *Eco*RV protein during its reactions with an oligodeoxynucleotide: one causing an increase in fluorescence upon DNA binding in either the absence or presence of Mg^{2+} (Figure 1A,B); a second, again increasing the fluorescence, upon the binding of Mg^{2+} to the preformed enzyme−DNA complex (Figure 4B); a third, resulting in a decrease in fluorescence, concomitant with phosphodiester hydrolysis (Figures 1D and 4C). The rates of all three of these processes were measured by stopped-flow fluorescence across a range of concentrations of $MgCl_2$, from 0.25 to 6 mM. The rate constants for the first process were found to be invariant with the concentration of $MgCl_2$ (data not shown), but the rates for both the second and third varied with the concentration of $MgCl_2$ (Figure 5).

The intermediate rate of fluorescence enhancement, observed only after the addition of Mg^{2+} to a preformed enzyme−DNA complex (Figure 4B), showed a complicated dependence on concentration of $MgCl_2$ (Figure 5A). We can account for the decrease in this rate as the concentration of Mg^{2+} ions is raised from 0.25 to 2.0 mM on a reaction scheme with a slow unimolecular step followed by a rapid bimolecular step:

$$ES\dagger \underset{k_{-1}}{\overset{k_1}{\rightleftharpoons}} ES\ddagger \overset{\pm M}{\Longrightarrow} EMS\ddagger \qquad (4)$$

where † and ‡ represent states with partial and full enhancements of protein fluorescence, respectively, and M the Mg^{2+} ion. On this scheme, the apparent rate constant for the formation of EMS‡ falls from $k_1 + k_{-1}$ at low Mg^{2+} levels to just k_1 at high levels (Halford, 1971; Fersht, 1985). We can also account for the increase in rate at $MgCl_2$ concentrations >2 mM on a reaction scheme with a fast bimolecular step followed by a slow unimolecular step:

$$ES\dagger + M \rightleftarrows EMS\ddagger \underset{k_{-2}}{\overset{k_2}{\rightleftharpoons}} EMS\ddagger \qquad (5)$$

On this second scheme, the apparent rate constant for EMS‡ formation rises from k_{-2} to $k_2 + k_{-2}$ as the level of Mg^{2+} is increased (Halford, 1971; Gutfreund, 1972). However, we have been unable to find a single scheme that can account for the complete Mg^{2+} profile. Perhaps the Mg^{2+}-induced conversion of the nonproductive enzyme−DNA complex to the productive complex can proceed by two or more alternative pathways, with the major routes being eq 4 at low Mg^{2+} levels and eq 5 at high Mg^{2+} levels.

The apparent rate constants for the fluorescence decay increased linearly with the concentration of $MgCl_2$ (Figure 5B). The decay phase has been correlated to phosphodiester hydrolysis (Figure 2) at a rate defined by k_h (eq 1). But the difference between the Mg^{2+} dependencies for phosphodiester hydrolysis (Figure 5B) and for the generation of the enzyme−Mg^{2+}−DNA complex (Figure 5A) demonstrates that the formation of the latter complex is not by itself sufficient to allow for DNA cleavage: the enzyme−Mg^{2+}−DNA complex still needs to bind additional Mg^{2+} before it can cleave DNA. The Mg^{2+} dependency for the fluorescence decay (Figure 5B) can be accounted for by proposing that the initial enzyme−Mg^{2+}−DNA complex, EMS‡, binds the Mg^{2+} ion that is required for phosphodiester hydrolysis (thus forming an intermediate containing Mg^{2+} at two separate sites, denoted as EMSM‡) with a K_D value that is much higher than the highest concentration of Mg^{2+} used here. From the reaction scheme

$$EMS\ddagger + M \overset{K_D}{\rightleftharpoons} EMSM\ddagger \overset{k_2}{\longrightarrow} EPM \qquad (6)$$

it follows that, provided the initial equilibration governed by K_D is faster than the cleavage step and that the concentration of M is higher than the EMS‡ complex, then

$$k_h = k_2([M]/\{[M] + K_D\}) \qquad (7)$$

Thus, whenever $K_D \gg [M]$, k_h will increase linearly with increasing [M].

Significantly, there are two Mg^{2+}-dependent steps in the *Eco*RV reaction. The first involves the incorporation of Mg^{2+} into the enzyme−DNA complex to form the precatalytic ternary complex, the species with the maximally enhanced fluorescence. The second is phosphodiester hydrolysis. The two Mg^{2+}-dependent steps are, however, distinct from each other both kinetically, in that they occur over different time scales (Figure 4, panels B and C), and thermodynamically, in that they have different Mg^{2+} dependencies (Figure 5A,B). This eliminates the possibility that both processes are controlled by the same Mg^{2+} ion at the same location in the active site of *Eco*RV. Instead, they must be due to different Mg^{2+} ions at different locations. These results are consistent with the proposal in the preceding paper (Vipond et al., 1995) for two metal ions at each active

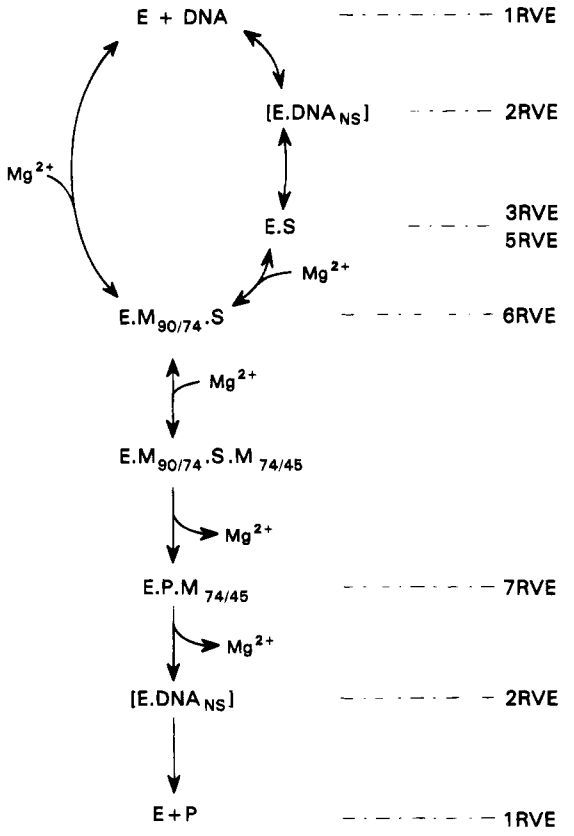

FIGURE 6: Structure–function correlation for *Eco*RV. The left-hand column lists the principal intermediates proposed here for the reaction mechanism of the *Eco*RV restriction endonuclease. This scheme reflects the catalytic events at one out of the two active sites in the dimeric protein, each of which cleaves one strand of the DNA (Winkler, 1992). The DNA contains both nonspecific sequences (DNA_{NS}) and an *Eco*RV recognition site (S) that is cleaved to product (P). The *Eco*RV enzyme (E) contains two binding sites for Mg^{2+} ions: one between Asp90 and Asp74 ($M_{90/74}$) and one between Asp74 and Glu45 ($M_{74/45}$). The right-hand column lists the PDB file names for the structures that have been determined for the *Eco*RV endonuclease, with and without DNA (Winkler et al., 1993) and also with and without divalent metal ions (Kostrewa & Winkler, 1995). Each structure has been aligned with a particular intermediate in the reaction pathway.

site, both participating in the catalytic reaction. By itself, the kinetic analysis in this study would also be consistent with the first Mg^{2+} that binds to the *Eco*RV-DNA complex, to form the EMS‡ intermediate, having purely a structural role. But the synergistic effects of metal ion combinations on *Eco*RV activity (Vipond et al., 1994) suggest that both metals have catalytic roles.

CONCLUSIONS

In this study, the application of rapid reaction techniques has resolved many of the individual steps in the reaction of the *Eco*RV endonuclease on a 12 bp oligodeoxynucleotide. The minimal reaction scheme that can account for both these observations, and also earlier studies on the kinetics of plasmid DNA cleavage by *Eco*RV (Halford et al., 1993; Vipond et al., 1995), is the pathway shown in Figure 6. Can we relate this mechanism to the structural data now available on the *Eco*RV restriction enzyme? To date, structures for the following states of *Eco*RV have been determined by X-ray crystallography (Winkler et al., 1993; Kostrewa & Winkler, 1995):

(a) The free protein in the absence of DNA and Mg^{2+} ions (Brookhaven PDB file 1RVE). In this state, the cleft between the two subunits of the dimer, where the DNA is located in the complex, is too narrow to accommodate DNA. In addition, the two peptide loops that form the principal contacts to the DNA in the complexes (the R- and Q-loops; Winkler et al., 1993) are disordered and appear to occupy the space that is eventually occupied by DNA.

(b) The protein bound to nonspecific DNA (2RVE). This structure contains two 8 bp DNA duplexes with sequences unrelated to the *Eco*RV site, stacked end-to-end in the cleft between the subunits. The conformation of the protein differs from that in the free protein while the DNA is close to B-form (Winkler et al., 1993).

(c) The protein bound to its recognition site in the absence of Mg^{2+} ions (3RVE, 4RVE, and 5RVE).[4] These again display a novel protein conformation with the R-loops wrapping over the DNA, thus surrounding the DNA with protein. They also display highly distorted DNA conformations. In the nonspecific complex, the B-DNA lies distant from the active site while the DNA distortion in the specific complex places the phosphate at the scissile bond close to Asp74 and Asp90 (Winkler et al., 1993; Kostrewa & Winkler, 1995).

(d) The protein bound to its recognition site in the presence of Mg^{2+} (6RVE). The metal ion is liganded to the phosphate at the scissile bond in the DNA and to the carboxylates from Asp90 and Asp74 (the 90/74 site). Even so, the cognate DNA remains intact: no DNA cleavage occurs in these co-crystals (Kostrewa & Winkler, 1995).

(e) An enzyme–product complex (7RVE). This was formed by crystallizing *Eco*RV after a DNA cleavage reaction in the presence of Mg^{2+} (Kostrewa & Winkler, 1995). The 5′-phosphate generated by DNA cleavage is positioned differently from the equivalent phosphodiester in the enzyme–substrate complex, and the 90/74 site for Mg^{2+} is no longer occupied by the metal ion. Instead, a Mg^{2+} between Asp74 and Glu45 (the 74/45 site) is liganded to one of the phosphoryl oxygens.

One could argue that the crystal structures of the enzyme–substrate–Mg^{2+} and enzyme–product–Mg^{2+} complexes are not true reflections of reaction intermediates since the former (6RVE) failed to cleave the DNA while the latter (7RVE) was generated by crystallization after the cleavage reaction so the positions of the reacting groups may not be the same as those following DNA cleavage *in situ*. But the following proposals permit the alignment of all five of these crystal structures with intermediates in the kinetic pathway (Figure 6).

First, the endonuclease must bind to DNA. The 12 bp DNA substrate used here is too short to allow for binding other than at the *Eco*RV recognition sequence. Our stopped-flow experiments therefore cannot provide any information about the role of nonspecific DNA in these reactions. From earlier studies with longer DNA molecules (Vipond & Halford, 1993), the initial binding will be almost certainly be at nonspecific DNA sequences. In the absence of Mg^{2+},

[4] The initial 3.0-Å model, 3RVE (Winkler et al., 1993), was further refined to yield the current Brookhaven entry, 4RVE (F. K. Winkler, personal communication), but a subsequent study with a DNA where the recognition site was flanked with a different sequence gave a structure at 2.0-Å resolution, 5RVE (Kostrewa & Winkler, 1995).

*Eco*RV binds DNA without any preference for its recognition site and specific binding is only observed in the presence of Mg^{2+} (Taylor et al., 1991; Thielking et al., 1992). On a long DNA, *Eco*RV can translocate from nonspecific to specific sites without dissociating from the DNA. The absence of facilitated diffusion on a 12 bp DNA is likely to be one of the reasons why this oligonucleotide is cleaved by *Eco*RV with different kinetics from plasmids, though a substrate with only 3 bp of DNA either side of the recognition site is also too short to meet all of the DNA binding functions in the protein. The activity of *Eco*RV is influenced by flanking sequences 4 bp away from the recognition site (Taylor & Halford, 1992).

DNA binding in the absence of Mg^{2+} can thus be described by 1RVE → 2RVE → 5RVE (Figure 6). Each of these states have altered protein structures (Winkler et al., 1993). However, we were unable to separate the kinetics of the bimolecular association of *Eco*RV with DNA from the conformational change that appears to be responsible for the enhanced tryptophan fluorescence. In other systems such as DNA polymerase I, conformational changes in DNA-protein complexes are often comparatively slow and well-separated from the bimolecular steps (Eger & Benkovic, 1992) For *Eco*RV, the initial conformational change is extremely rapid, even though it involves large alterations to both protein and DNA structures: opening the cleft between the subunits by altering the relative positions of domains in each polypeptide; repositioning and ordering the R- and Q-loops that contact the DNA; distorting the DNA from B-form (Winkler et al., 1993). Moreover, the specific complex formed in the absence of Mg^{2+} (5RVE) has to undergo an additional rearrangement on binding Mg^{2+} (Figure 4B). Strikingly, the latter rearrangement is absent from the reaction when DNA binds to *Eco*RV in the presence of Mg^{2+} (Figure 1C). Instead of generating the high fluorescence transient by DNA binding followed by Mg^{2+} binding, the reaction can proceed directly to the high fluorescence state. The stable *Eco*RV−DNA complexes formed in the absence of Mg^{2+} are therefore not on the main reaction pathway, though they can rejoin the pathway by an alternative route.

We suggest that the precatalytic ternary complex with maximally enhanced fluorescence, EMS‡ (eqs 4 and 5), is directly equivalent to 6RVE, i.e., the specific complex with Mg^{2+} at the 90/74 site but which fails to cleave DNA (Kostrewa & Winkler, 1995). We also suggest that the additional Mg^{2+} that must bind to this complex for phosphodiester hydrolysis is located at the 74/45 site (Vipond et al., 1995), i.e., at one of the positions for Mg^{2+} observed in the enzyme−product complex, 7RVE (Kostrewa & Winkler, 1995). In the enzyme−substrate complex, the 90/74 site is likely to have a high affinity for Mg^{2+}, since the ion is liganded by two aspartates and by the phosphodiester, leaving only three water molecules to complete the octahedral coordination. In contrast, the 74/45 site may have a low affinity: if a divalent metal ion is placed at this site in 6RVE, it would be liganded by only two fixed groups, the carboxylates from Asp74 and Glu45, and it would need four water molecules for octahedral geometry. This proposal can account for why the precatalytic ternary complex, EMS‡, can be formed with a low concentration of Mg^{2+} (Figure 5A) while the formation of the catalytically competent complex, EMSM‡, requires higher concentrations of Mg^{2+} (Figure 5B).

The relative affinities of the 90/74 and the 74/45 sites for Mg^{2+} will, however, be reversed in the enzyme−product complex. In 7RVE, the 5'-phosphate at the site of cleavage lies over the 74/45 site instead of the 90/74 site (Kostrewa & Winkler, 1995). Consequently, following both the hydrolytic reaction that converts the phosphodiester to a phosphomonoester and the associated movement of that phosphate, a Mg^{2+} at the 90/74 site would be free to dissociate from the protein. This scheme provides an explanation for why the crystals of *Eco*RV have a metal ion at the 90/74 site in the enzyme−substrate complex and at the 74/45 site in the enzyme−product complex. Hence, it can account for the conversion of 6RVE to 7RVE.

All five of the states of the *Eco*RV restriction enzyme that have been characterized by X-ray crystallography can thus be correlated with an intermediate in the reaction pathway (Figure 6). Moreover, the minimal reaction pathway for *Eco*RV requires only one intermediate for which a crystal structure has yet to be determined. In order to accommodate both the kinetic analysis in this report and the synergism between different metal ions described in the previous paper (Vipond et al., 1995), we propose an additional intermediate in which metal ions are bound simultaneously to both the 90/74 and the 74/45 sites at the catalytic center of *Eco*RV (Figure 6). The additional intermediate appears to be responsible for phosphodiester hydrolysis, presumably by a two-metal mechanism of the type proposed by Steitz (1993).

ACKNOWLEDGMENT

We thank Bernard Connolly, Symon Erskine, Freddie Gutfreund, Alfred Pingoud, Mark Szczelkun, and Fritz Winkler for discussions and for unpublished data. This work was initiated while S.E.H. held a Royal Society Leverhulme Trust Senior Research Fellowship.

REFERENCES

Alves, J., Urbanke, C., Fliess, A., Maass, G., & Pingoud, A. (1989) *Biochemistry 28*, 7879−7888.

Baldwin, G. S., & Halford, S. E. (1994) *Biochem. Soc. Trans. 22*, 300S.

Craig, M. E., & Crowthers, D. M. (1971) *J. Mol. Biol. 62*, 383−401.

D'Arcy, A., Brown, R. S., Zabeau, M., van Resandt, R. W., & Winkler, F. W. (1985) *J. Biol. Chem. 260*, 1987−1990.

Eger, B. T., & Benkovic, S. J. (1992) *Biochemistry 31*, 9227−9236.

Fersht, A. R. (1985) *Enzyme Structure and Mechanism*, 2nd ed., W. H. Freeman, New York.

Grasby, J., & Connolly, B. A. (1992) *Biochemistry 31*, 7855−7861.

Gutfreund, H. (1972) *Enzymes: Physical Principles*, John Wiley, London.

Halford, S. E. (1971) *Biochem. J. 125*, 319−327.

Halford, S. E., & Johnson, N. P. (1983) *Biochem. J. 211*, 405−415.

Halford, S. E., & Goodall, A. J. (1988) *Biochemistry 27*, 1771−1777.

Halford, S. E., Taylor, J. D., Vermote, C. L. M., & Vipond, I. B. (1993) in *Nucleic Acids and Molecular Biology* (Eckstein, F., & Lilley, D. M. J., Eds.) Vol. 7, pp 47−69, Springer-Verlag, Berlin.

Jeltsch, A., Alves, J., Wolfes, H., Maass, G., & Pingoud, A. (1993) *Proc. Natl. Acad. Sci. U.S.A. 90*, 8499−8503.

Kostrewa, D., & Winkler, F. K. (1995) *Biochemistry* (first paper of three in this issue).

Lohman, T. M. (1986) *CRC Crit. Rev. Biochem. 19*, 191−245.

Luke, P. A., McCallum, S. A., & Halford, S. E. (1987) *Gene Amplif. Anal. 5*, 183−205.

Newman, P. C., Nwosu, V, U., Williams, M. D., Cosstick, R., Seela, F., & Connolly, B. A. (1990a) *Biochemistry 29*, 9891−9901.

Newman, P. C., Williams, M. D., Cosstick, R., Seela, F., & Connolly, B. A. (1990b) *Biochemistry 29*, 9902−9910.

Schildkraut, I., Banner, C. D., Rhodes, C. S., & Parekh, S. (1984) *Gene 27*, 327−329.

Selent, U., Rüter, T., Köhler, E., Liedtke, M., Thielking, V., Alves, J., Oelgeschläger, T., Wolfes, H., Peters, F., & Pingoud, A. (1992) *Biochemistry 31*, 4808−4815.

Steitz, T. A. (1993) *Curr. Opin. Struct. Biol. 3*, 31−38.

Taylor, J. D., & Halford, S. E. (1989) *Biochemistry 28*, 6198−6207.

Taylor, J. D., & Halford, S. E. (1992) *Biochemistry 31*, 90−97.

Taylor, J. D., Badcoe, I. G., Clarke, A. R., & Halford, S. E. (1991) *Biochemistry 30*, 8743−8753.

Terry, B. J., Jack, W. E., & Modrich, P. (1987) *Gene Amplif. Anal. 5*, 103−118.

Thielking, V., Selent. U., Köhler, E., Wolfes, H., Pieper, U., Geiger, R., Urbanke, C., Winkler, F. K., & Pingoud, A. (1991) *Biochemistry 30*, 6416−6422.

Thielking, V., Selent. U., Köhler, E., Landgraf, A., Wolfes, H., Alves, J., & Pingoud, A. (1992) *Biochemistry 31*, 3727−3732.

Vermote, C. L. M., & Halford, S. E. (1992) *Biochemistry 31*, 6082−6089..

Vermote, C. L. M., Vipond, I. B., & Halford, S. E. (1992) *Biochemistry 31*, 6089−6097.

Vipond, I. B., & Halford, S. E. (1993) *Mol. Microbiol. 9*, 225−231.

Vipond, I. B., Baldwin, G. S., & Halford, S. E. (1995) *Biochemistry* (second paper of three in this issue).

Waters, T. R., & Connolly, B. A. (1992) *Anal. Biochem. 204*, 204−209.

Waters, T. R., & Connolly, B. A. (1994) *Biochemistry 33*, 1812−1819.

Winkler, F. K. (1992) *Curr. Opin. Struct. Biol. 2*, 93−99.

Winkler, F. K., Banner, D. W., Oefner, C., Tsernoglou, D., Brown, R. S., Heathman, S. P., Bryan, R. K., Martin, P. D., Petratos, K., & Wilson, K. S. (1993) *EMBO J. 12*, 1781−1795.

BI941628N